ANTIOXIDANTS & REDOX SIGNALING
Volume 20, Number 8, 2014

DOI: 10.1089/ars.2013.5366

Therapeutics

ORIGINAL RESEARCH COMMUNICATION

Hemojuvelin Modulates Iron Stress During Acute Kidney Injury: Improved by Furin Inhibitor

Guang-Huar Young,[1] Tao-Min Huang,[2] Che-Hsiung Wu,[3] Chun-Fu Lai,[4] Chun-Cheng Hou,[5] Kang-Yung Peng,[4] Chan-Jung Liang,[6] Shuei-Liong Lin,[4] Shih-Chung Chang,[7] Pi-Ru Tsai,[1] Kwan-Dun Wu,[4] Vin-Cent Wu,[4] Wen-Je Ko,[1,8] and the NSARF group[9]

Abstract

Aims: Free iron plays an important role in the pathogenesis of acute kidney injury (AKI) *via* the formation of hydroxyl radicals. Systemic iron homeostasis is controlled by the hemojuvelin-hepcidin-ferroportin axis in the liver, but less is known about this role in AKI. ***Results:*** By proteomics, we identified a 42 kDa soluble hemojuvelin (sHJV), processed by furin protease from membrane-bound hemojuvelin (mHJV), in the urine during AKI after cardiac surgery. Biopsies from human and mouse specimens with AKI confirm that HJV is extensively increased in renal tubules. Iron overload enhanced the expression of hemojuvelin-hepcidin signaling pathway. The furin inhibitor (FI) decreases furin-mediated proteolytic cleavage of mHJV into sHJV and augments the mHJV/sHJV ratio after iron overload with hypoxia condition. The FI could reduce renal tubule apoptosis, stabilize hypoxic induced factor-1, prevent the accumulation of iron in the kidney, and further ameliorate ischemic-reperfusion injury. mHJV is associated with decreasing total kidney iron, secreting hepcidin, and promoting the degradation of ferroportin at AKI, whereas sHJV does the opposite. ***Innovation:*** This study suggests the ratio of mHJV/sHJV affects the iron deposition during acute kidney injury and sHJV could be an early biomarker of AKI. ***Conclusion:*** Our findings link endogenous HJV inextricably with renal iron homeostasis for the first time, add new significance to early predict AKI, and identify novel therapeutic targets to reduce the severity of AKI using the FI. *Antioxid. Redox Signal*. 20, 1181–1194.

Introduction

Acute kidney injury (AKI) is a serious complication in hospitals, resulting in a prolonged hospital stay and high mortality (7). Despite recent advances in clinical care, the mortality associated with AKI remains high, ranging from 20% to 60% in hospitalized patients (36). During AKI, the kidney injury is subjected to excess iron from degraded red blood cells and cytochrome P-450s (2, 5) The free iron is involved in the generation of reactive oxygen species (ROS) *via* the Haber–Weiss and Fenton reactions (38), whereby the superoxide radical and hydrogen peroxide yield the hydroxyl radical (12). Iron plays a critical role in mediating kidney tubular injury *via* the generation of the hydroxyl radical or a similar oxidant (11). Increased free radical reactions are catalyzed by catalytic iron, which has been demonstrated in

[1]Department of Surgery, National Taiwan University Hospital, Taipei, Taiwan.
[2]Division of Nephrology, Department of Internal Medicine, Yun-Lin Branch, National Taiwan University Hospital, Douliou City, Taiwan.
[3]Division of Nephrology, Buddhist Tzu Chi General Hospital, Taipei Branch, Taiwan.
[4]Division of Nephrology, Department of Internal Medicine, National Taiwan University Hospital, Taipei, Taiwan.
[5]Department of Internal Medicine, Min-Sheng General Hospital, Tao-Yuan, Taiwan.
[6]Department of Anatomy and Cell Biology, National Taiwan University, Taipei, Taiwan.
[7]Department of Biochemical Science and Technology, College of Life Sciences, National Taiwan University, Taipei, Taiwan.
[8]Department of Traumatology, National Taiwan University Hospital, Taipei, Taiwan.
[9]NSARF: The National Taiwan University Study Group on Acute Renal Failure.

Innovation

Free iron plays important roles in models of ischemic and toxic acute kidney injury (AKI) through generation of oxygen free radicals. The regulation of hemojuvelin-hepcidin-ferroportin axis is associated with excess of free heme and iron. Hypoxia-based kidney injury directly activates furin protease to release soluble hemojuvelin (sHJV), which in turn inhibits hepcidin activation, induces ferroportin, and impairs iron homeostasis. The present studies demonstrate that furin inhibitor decreases sHJV and ferroportin expression and abolishes iron deposition in kidney injury *in vivo*. Thus, sHJV not only serves as an early biomarker for AKI but also provides a renoprotective strategy with novel therapeutic potential.

several animal models of AKI (2, 4), and iron chelators including deferoxamine (DFO) and 2,3-dihydroxybenzoic acid could reduce the associated injury (26, 37). Free iron-related, ROS-mediated kidney injury appears to be the consistent pathophysiological connection for AKI biomarkers (11). Recently, identified biomarkers, including neutrophil gelatinase-associated lipocalin (NGAL) (23), liver-type fatty acid-binding protein (35), and alpha-1 microglobulin (8), predict the development of AKI and reflect both iron and heme metabolism (24). Further, hepcidin, a biomarker of AKI that develops after cardiopulmonary bypass, has been shown to play a pivotal role in the feedback mechanism by binding to an iron transporter ferroportin, thus leading to the degradation of ferroportin (14).

Among the proteins involved in iron homeostasis, hemojuvelin (HJV) is the key regulator of hepcidin expression (25, 28). HJV exists as a 50 kDa membrane-bound form (mHJV) and a 42 kDa soluble form (sHJV), which work as a reciprocal role in response to iron status (1). HJV plays a crucial role in iron absorption and release from cells and has anti-inflammatory properties, specifically in the iron-sensing pathway (34). The administration of sHJV in mice decreases the expression of hepcidin and causes iron deposition in the liver and blood (1). Although HJV mutation in mice could cause severe iron overload in the kidney (25), the role of kidney HJV during AKI has not been elucidated.

Using a proteomics approach, we first showed kidney HJV plays a vital role in iron homeostasis during AKI *in vivo* and *in vitro* and that the reciprocal functions of HJV depend on the presence of either mHJV or sHJV, which is the cleavage product of the furin protease (33). Moreover, the administration of a furin inhibitor (FI) could repress iron deposition, suppress tubular apoptosis, and finally, ameliorate renal injury.

Results

Comparison of the urinary protein patterns from AKI patients using proteomic methods

The urine pooled from 15 healthy volunteers and 15 post-cardiac surgery patients with or without AKI were compared (Fig. 1A). Among the identified protein spots from post-operative, two-dimensional electrophoresis (2-DE) maps, most of the upregulated spots were assigned to proteins associated with the transport or metabolism of iron (Supplementary Table S1; Supplementary Data are available online at www.liebertpub.com/ars). To confirm the target protein, the 2-DE of urinary proteins from pre- and post-ischemia/reperfusion (I/R), acute tubular necrosis (ATN) rats were also separated and transferred to a PVDF membrane. Of the urinary protein spots identified from the AKI patients and involved in iron metabolism, only the protein detected by the anti-HJV antibody increased in the ATN rats. To validate the novel biomarker, a specific anti-HJV antibody was also used to determine the major 42 kDa urinary proteins from ATN rats (Fig. 1B). Therefore, we selected HJV as a candidate biomarker for further validation.

The expression of HJV on AKI model

Twelve hours after C57BL/6 mice were subjected to I/R injury, the blood urea nitrogen (BUN) (131.67 ± 19.63 *vs.* 29.50 ± 5.84 mg/dl, $p < 0.01$) and serum creatinine (Scr) (1.26 ± 0.15 *vs.* 0.1667 ± 0.05 mg/dl, $p < 0.01$) were significantly elevated compared with those of the sham-operated controls. The levels of BUN and Scr were elevated after 3 h, reached a significant difference at 12 to 24 h and declined after 48 h (Fig. 2A). Tubular injury was scored on periodic acid-Schiff (PAS) stained kidney section (Supplementary Fig. S1). The scores from AKI mice were defined based on the percentage of tubules with cast formation, dilation, or necrosis as detailed in Materials and Methods section (Fig. 2B).

The kidney iron content increased after kidney I/R injury using Prussian stain (Fig. 2C). Immunohistochemical (IHC) analysis showed that HJV was widely expressed both in the cortex and in the medulla following an I/R injury, especially in the tubular cells (Fig. 2D). To explore the temporal changes in HJV in kidneys during AKI, HJV was compared with the iron-related biomarker NGAL (23), a downstream regulator of hepcidin and iron exporter of ferroportin (25). Western blot analysis (Fig. 2E) showed that the sHJV rapidly increased at 3 h, whereas the mHJV gradually increased after 24 h in the kidney. Likewise, the kidney injury marker NGAL (23) appeared later at 3–24 h (Fig. 2G). The mHJV/sHJV ratio had increased significantly at 24 h in the kidney, but did not change significantly over time in the liver (Fig. 2F). After the acute episode, hepcidin was augmented, accompanied by the withdrawal of ferroportin from the cell surface (Fig. 2G).

Consistent with the elevation of sHJV and ferroportin, an inductively coupled plasma atomic emission spectroscopy (ICP-AES) analysis indicated that AKI resulted in iron deposition in the kidney at 3 h (31.94 ± 4.15 *vs.* 81.16 ± 1.36 mg/kg, $p < 0.01$) compared with that of the sham-operated mice and declined after 48 h (Fig. 2H). The total kidney iron content after AKI significantly correlated to the ratio of mHJV/sHJV (Supplementary Fig. S3) (spearman correlation, $r = -0.851$, $p < 0.001$).

Moreover, in the early phase (3 h) of post I/R injury we observed the appearance of sHJV in plasma (Fig. 2I) and urine (Fig. 2J). The trichloroacetic acid (TCA)-precipitated urinary protein showed that urinary sHJV could also be incorporated into the band at 42 kDa, which appeared at 3 h as observed in the I/R rats (Fig. 1B).

Expression of HJV in the kidney tubule during AKI

After I/R injury (Fig. 3A), immunofluorescence staining demonstrated enhanced expression of HJV (red color) in epithelial cells, co-localized with lotus tetragonolobus lectin

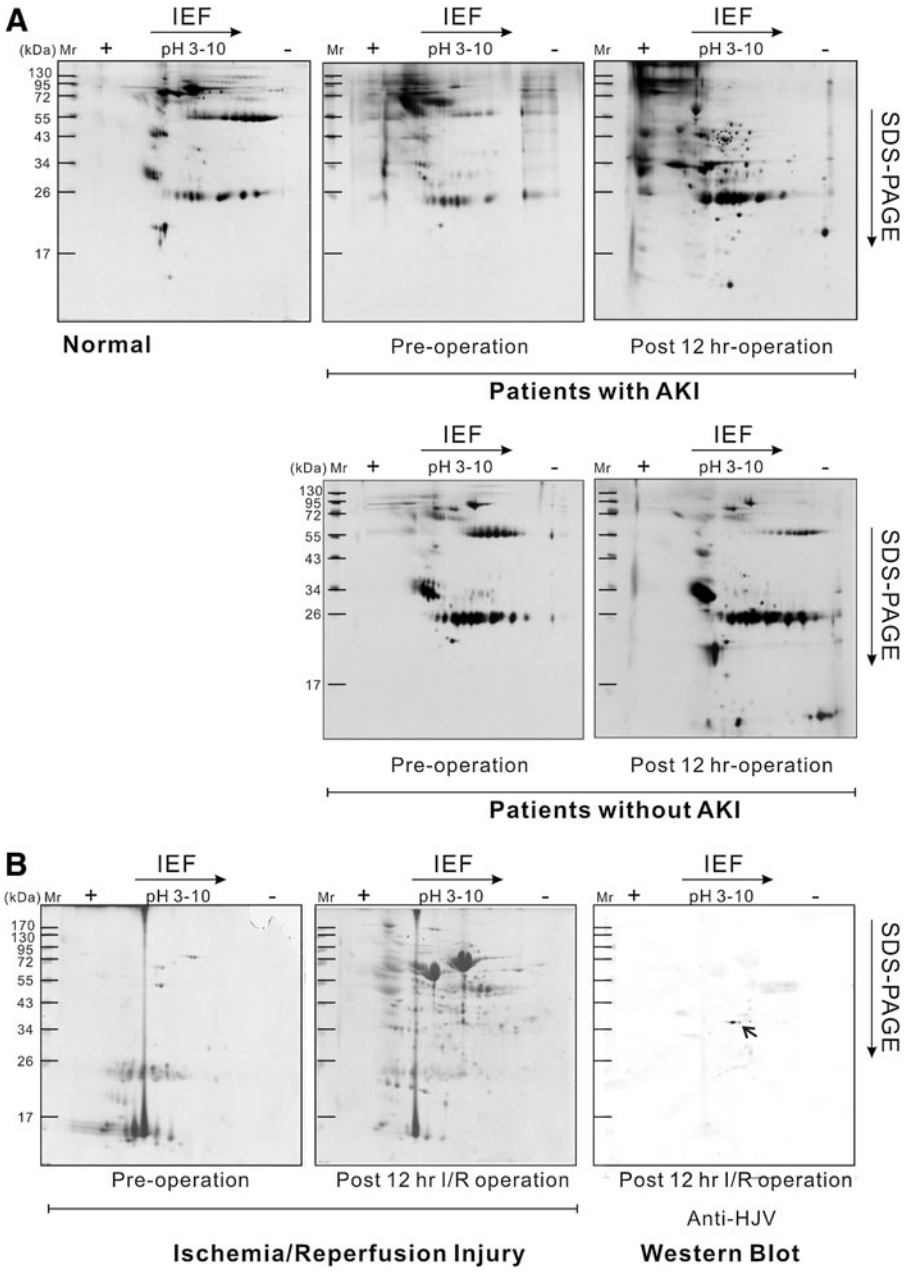

FIG. 1. The identification of urinary hemojuvelin by proteomic methods. (A) The comparison of urinary proteins from pooled urine samples from healthy volunteers, post-cardiac surgery patients with and without AKI using 2-DE maps, respectively. Protein spot identified as HJV is labeled in a dotted circle. **(B)** 2-DE maps of pooled urinary proteins from pre- and post-ischemia/reperfusion (I/R) injury rats. The gels were stained with Coomassie blue R250, transferred into a PVDF membrane, and developed using a polyclonal antibody against HJV (*arrow*). Significant changes in spots were processed and analyzed using LC-MS/MS as described. 2-DE, two-dimensional electrophoresis.

(green color) and dolichos biflorus agglutinin (yellow color) in mice. The increased HJV protein was widely observed on the epithelial surface of the proximal tubule of the cortex.

Likewise, kidney biopsies from human AKI showed higher expression of HJV in the renal tubule than the normal regions of renal cell carcinoma patients according to IHC (Fig. 3B). In light of this, HJV expression was localized to the injured tubules with obvious features of cast formation, tubular dilation, and tubular necrosis under the most intense hematoxylin and eosin (H&E) staining.

Elevated urinary sHJV during AKI

To validate the expression of urinary sHJV, we compared the urinary HJV and NGAL in various clinical scenarios. Urine was collected from 19 patients (Scr 4.11 ± 2.81 mg/dl) with established AKI and classified according to the AKIN stages 3 h after cardiovascular operation (22). Urine samples were also collected from 6 rhabdomyolysis patients with AKI (Scr 2.98 ± 1.61 mg/dl), 7 rhabdomyolysis patients without AKI (Scr 0.88 ± 0.15 mg/dl), 7 patients with established chronic kidney disease (CKD) (Scr 2.51 ± 1.15 mg/dl), 10 urinary tract infection (UTI) patients (Scr 1.45 ± 1.27 mg/dl), 14 patients (Scr 1.2 ± 0.5 mg/dl) with glomerulopathy, and 11 healthy volunteers (Scr, 0.8 ± 0.05 mg/dl). Figure 4 shows that the urinary HJV concentrations in the rhabdomyolysis patients with AKI (898.01 ± 213.03 ng/ml; $n = 6$) and those in the post-operative AKI group (265.8 ± 109.6 ng/ml; $n = 19$) were higher than those of the healthy volunteers (47.5 ± 16.5 ng/ml; $n = 11$), the CKD patients (88.68 ± 49.22 ng/ml; $n = 7$), the UTI patients (58.45 ± 62.8 ng/ml; $n = 10$), the GN patients

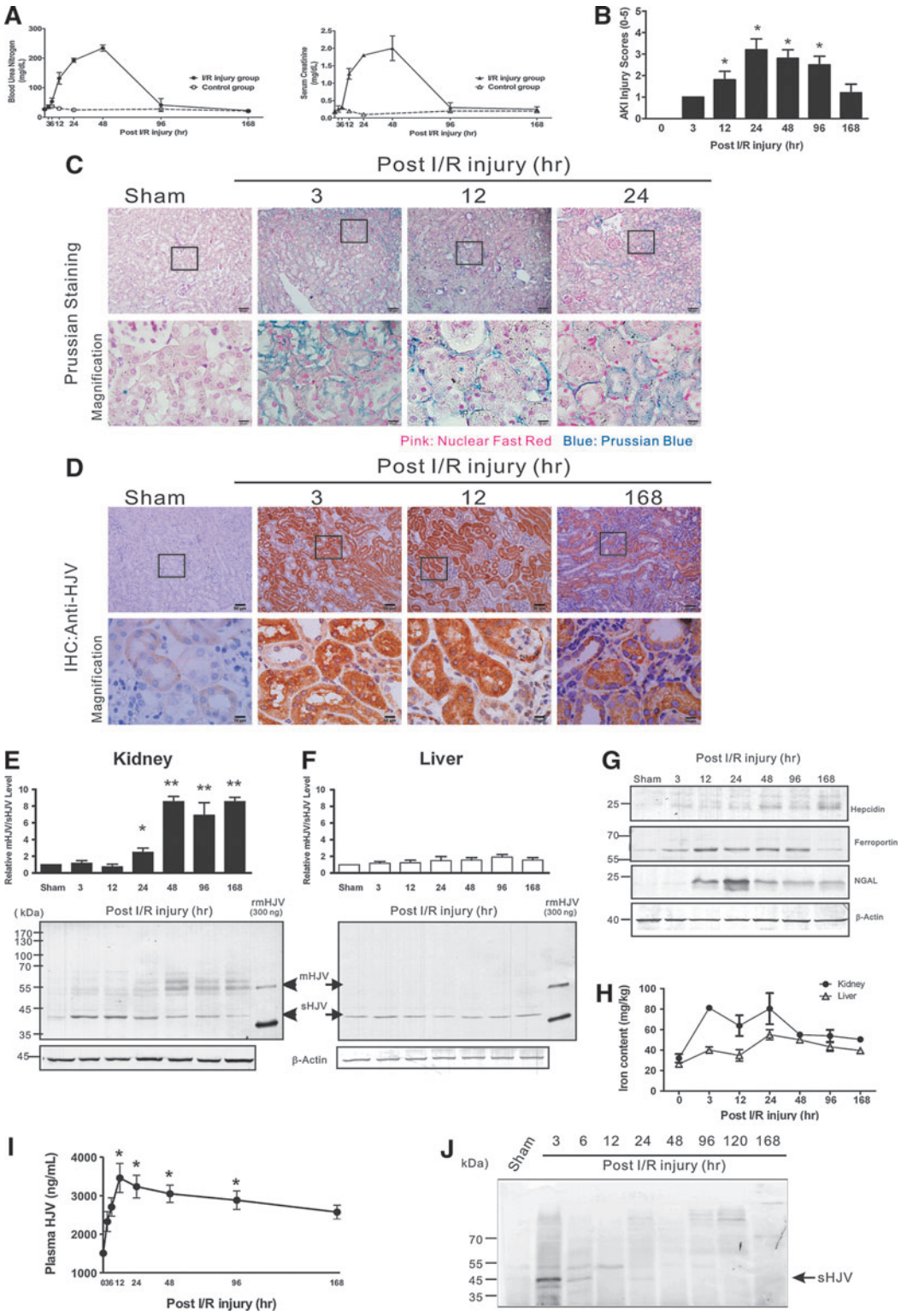

FIG. 2. Temporal change of HJV in renal I/R injury. (A) Change in serum creatinine and blood urea nitrogen (BUN) at different time points in mice. ($n=10$ at each time point). **(B)** Disease severity after I/R injury was shown by tubular injury score according to periodic acid–Schiff (PAS)-stained renal section at each time point. **(C)** Kidney sections stained with Prussian blue in terms of iron content. **(D)** Immunohistochemical (IHC) analysis using anti-HJV antibody (scale bars: 50 μM). **(E)** A representative western blot (30 μg/well) for membrane-bound hemojuvelin/soluble hemojuvelin (mHJV/sHJV) ratios from the total kidney and **(F)** liver lysate $^{**}p<0.01$ vs. sham (n=10). Typical results of 10 independent experiments are shown. Each experiment was normalized with the sham group and 300 ng recombinant mouse HJV (rmHJV) proteins, which produced bands at 57 and 38 kDa. **(G)** Kidney lysates at each time point were analyzed using anti-hepcidin, anti-ferroportin, and anti- neutrophil gelatinase-associated lipocalin (NGAL) antibodies. **(H)** Total kidney and liver iron concentration measured after renal I/R injury. The total iron was measured using inductively coupled plasma atomic emission spectroscopy (ICP-AES) analysis. **(I)** Temporal excretion of plasma HJV measured using ELISA and **(J)** Trichloroacetic acid/acetone precipitated urinary protein for western analysis using anti-HJV antibody. Urinary HJV was observed predominantly as sHJV (42 kDa), with lower amounts of mHJV (50 kDa) ($^{*}p<0.05$). To see this illustration in color, the reader is referred to the web version of this article at www.liebertpub.com/ars

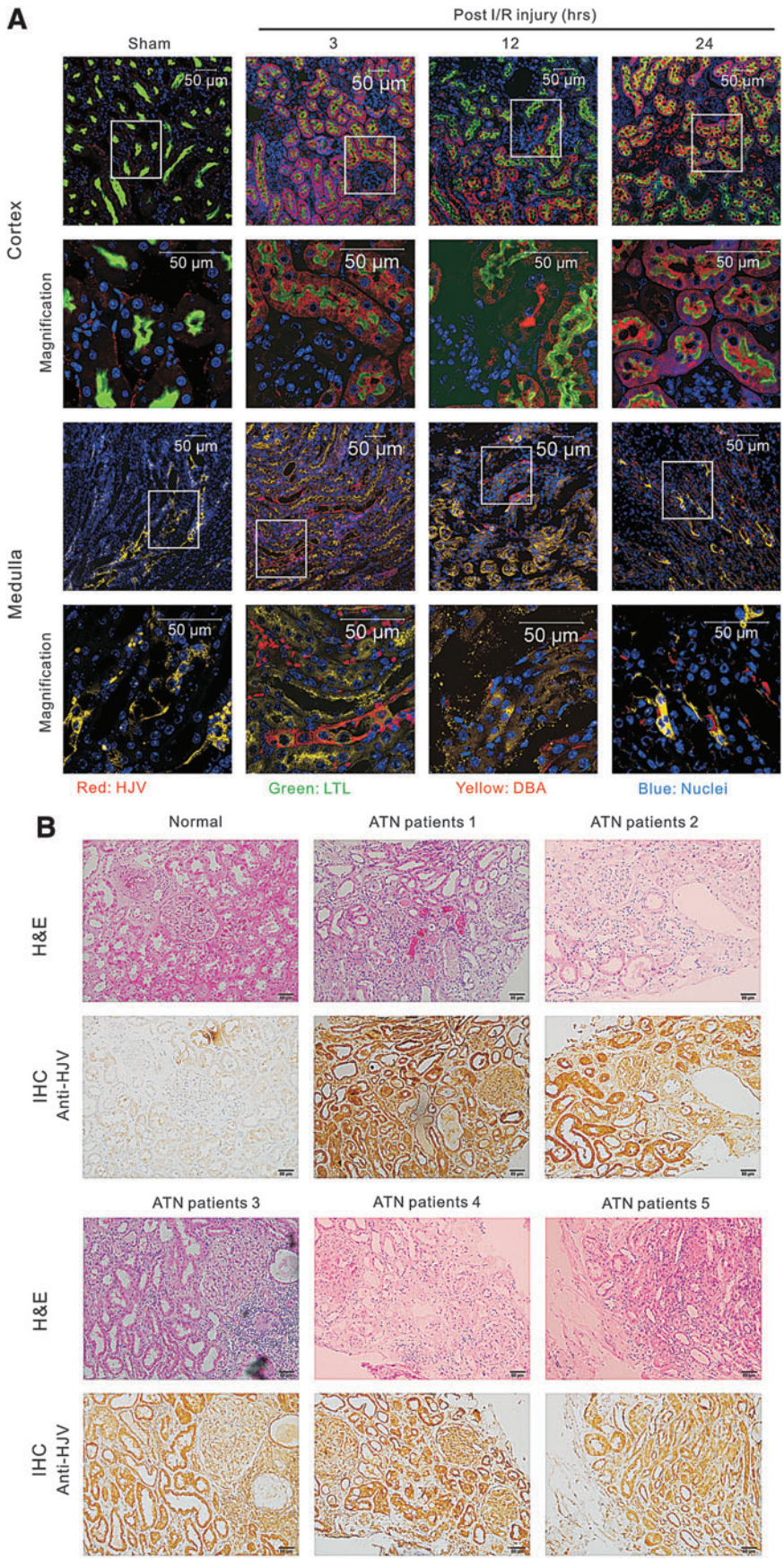

FIG. 3. Increase in expression of HJV in the cortical renal tubules in mice and humans after AKI. (A) In mice, increased HJV after renal I/R injury was predominantly in the renal tubules. **(B)** The staining of HJV in the normal human kidney cortex was less apparent; however, HJV was prominent in the renal tubules after hypovolemic shock-related AKI. The staining was homogenous and predominant in the proximal renal tubules. The histological images display five patients with acute tubular necrosis (ATN, patients 1–5), including fuzzy brush border, dilated renal tubule, and relative denuded nucleus. Scale bars: 50 μM. To see this illustration in color, the reader is referred to the web version of this article at www.liebertpub.com/ars

(157.15 ± 74.99 ng/ml; $n = 14$) and the rhabdomyolysis patients without AKI (236.9 ± 156.7 ng/ml; $n = 7$). These data were consistent with urine NGAL expression.

Iron overload under hypoxic condition induced HJV expression and the FI attenuated mHJV degradation into the sHJV form

Human proximal renal tubule HK2 cells were pretreated with a furin protease inhibitor, the iron chelator DFO, or the recombinant human HJV protein (rhHJV), and then were subsequently added to 100 μM ferric chloride ($FeCl_3$) accompanied with 1% oxygen for 24 h to mimic iron overload and hypoxia conditions (44). To distinguish the secreted sHJV from HK2 cells, the culture media were incubated with an anti-HJV monoclonal antibody for an immunoprecipitation (IP) assay, and the bound complex containing sHJV, which is released from HK2 cells, was identified using an anti-HJV polyclonal antibody (Supplementary Fig. S4). Iron overload and hypoxia (Fig. 5A) could promote the expression of HJV markedly. Hypoxic-induced factor-1 (HIF-1) elevated after adding DFO or under hypoxic condition, however, it was restored after adding FI. Pretreatment with FI could enhance the expression of mHJV, whereas, DFO and rhHJV have less impact on the induction of mHJV in HK2 cells (Fig. 5A and Supplementary Fig. S4A).

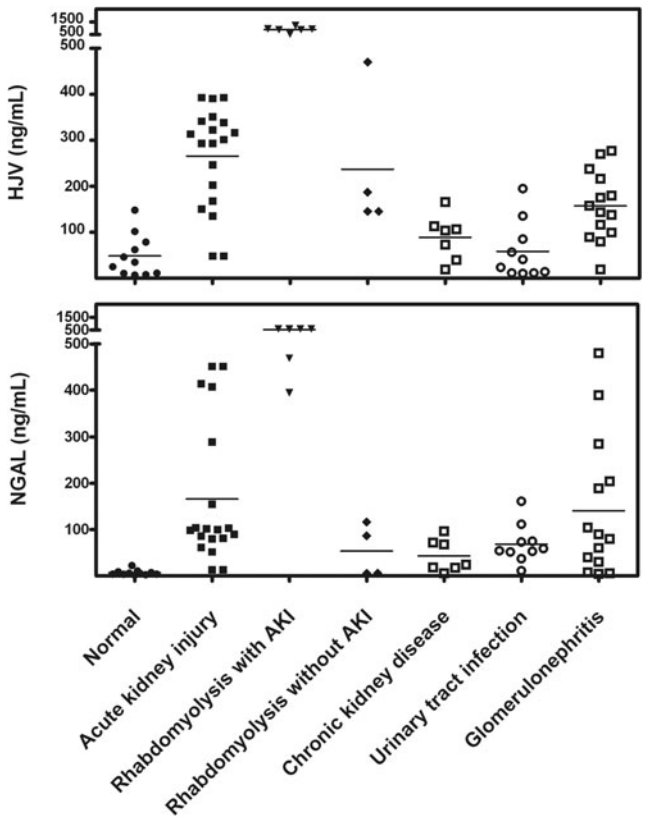

FIG. 4. Expression of urinary HJV and NGAL in different kidney diseases of patients. Human urine samples from patients after cardiac surgery and rhabdomyolysis-related AKI exhibited high levels of HJV, whereas samples from patients with chronic kidney disease (CKD), glomerulonephropathy, and urinary tract infection exhibited a low level of HJV, as detected by an ELISA. These results were similar to those obtained for urine NGAL expression.

Prussian blue staining of HK2 cells revealed that both FI and DFO could diminish iron deposition but rhHJV perturb iron accumulation more seriously (Fig. 5C).

Amelioration of I/R injury, iron deposition, and tubular apoptosis in kidney by a FI

To determine the role of iron homeostasis involving HJV during AKI, we next examined the rescue effects of the FI and the role of sHJV in iron deposition using an I/R model.

Renal I/R injury induced a rapid loss of renal function, as indicated by the increasing levels of BUN and Scr, which was ameliorated in animals pretreated with the FI (BUN 192.75 ± 7 *vs.* 47.53 ± 20 mg/dl; Scr 1.8 ± 0.1 *vs.* 0.3 ± 0.08 mg/dl, $p = 0.05$ at 24 h, $n = 10$, all $p < 0.01$). In light of this, we detected no significant change in iron deposition in the liver (50.18 ± 7.88 *vs.* 37.2 ± 10.6 mg/kg at 24 h, $n = 10$, $p = 0.04$); the total iron content in the kidneys was declined (76.11 ± 15.14 *vs.* 43.21 ± 17.26 mg/kg at 24 h, $n = 10$, $p = 0.03$) in mice treated with FI compared with the results following a PBS injection before I/R (Fig. 6A). However, mice that received recombinant mouse HJV protein (rmHJV) before an I/R injury exhibited considerably increased iron deposition, especially in the kidney (155.25 ± 13.29 *vs.* 76.11 ± 15.14 mg/kg at 24 h, $n = 10$, $p = 0.04$ *vs.* I/R injury), but no significant change in deposition in the liver (47.39 ± 16.5 *vs.* 55.18 ± 7.09 mg/kg at 24 h, $n = 10$, $p = 0.64$ *vs.* I/R injury). This result suggested that excess rmHJV (sHJV) exacerbated iron deposition and that the FI diminished iron deposition in the kidney but not in the liver after kidney I/R. Likewise, the tubular injury score is corresponding to the renal function and iron deposition in I/R kidney (Fig. 6B and Supplementary Fig. S7).

Consistent with our *in vitro* data, FI decreased kidney iron content, enhanced mHJV, attenuated sHJV, increased the ratio of mHJV/sHJV, induced the expression of hepcidin, and then prompted the degradation of ferroportin, whereas rmHJV(sHJV) did the opposite (Fig. 6C). The kidney injury marker NGAL was augmented by rmHJV and downregulated by FI accordingly. Therefore, we speculated that the increased kidney sHJV is correlated with the excess heme iron derived from hemoglobin during AKI, and that the generation of sHJV is mediated by furin protease.

Further, the renal tubules of the apoptotic cell numbers were reduced by pretreatment with the FI ($p = 0.02$) and enhanced by adding rmHJV ($p = 0.01$), as observed *via* fluorescence staining ($p = 0.02$) (Fig. 6D). Importantly, iron deposition in kidney during AKI significantly correlate with the apoptosis severity as stained by tunnel-positive tubules (Pearson correlation, p = 0.045, r = 0.955). Quantitative evaluation of superoxide production by DHE staining showed FI could decrease the superoxide production (Fig. 6E).

To investigate whether the amelioration of FI in AKI mice is altered *via* the expression of HJV, we analyzed kidney lysates from wild-type and HJV knockout mice (15) that received I/R injury at post-24 h. Iron staining revealed that $HJV^{-/-}$ mice had a significant iron accumulation in renal tubules (Fig. 7A). Further, FI could restore mHJV, hepcidin, and decreased ferroportin and NGAL expression in wild-type mice at I/R kidney injury, whereas those were not found in $HJV^{-/-}$ mice (Fig. 7B).

Discussion

In this study, we showed evidence that kidney HJV plays an important role in iron homeostasis during AKI. We found

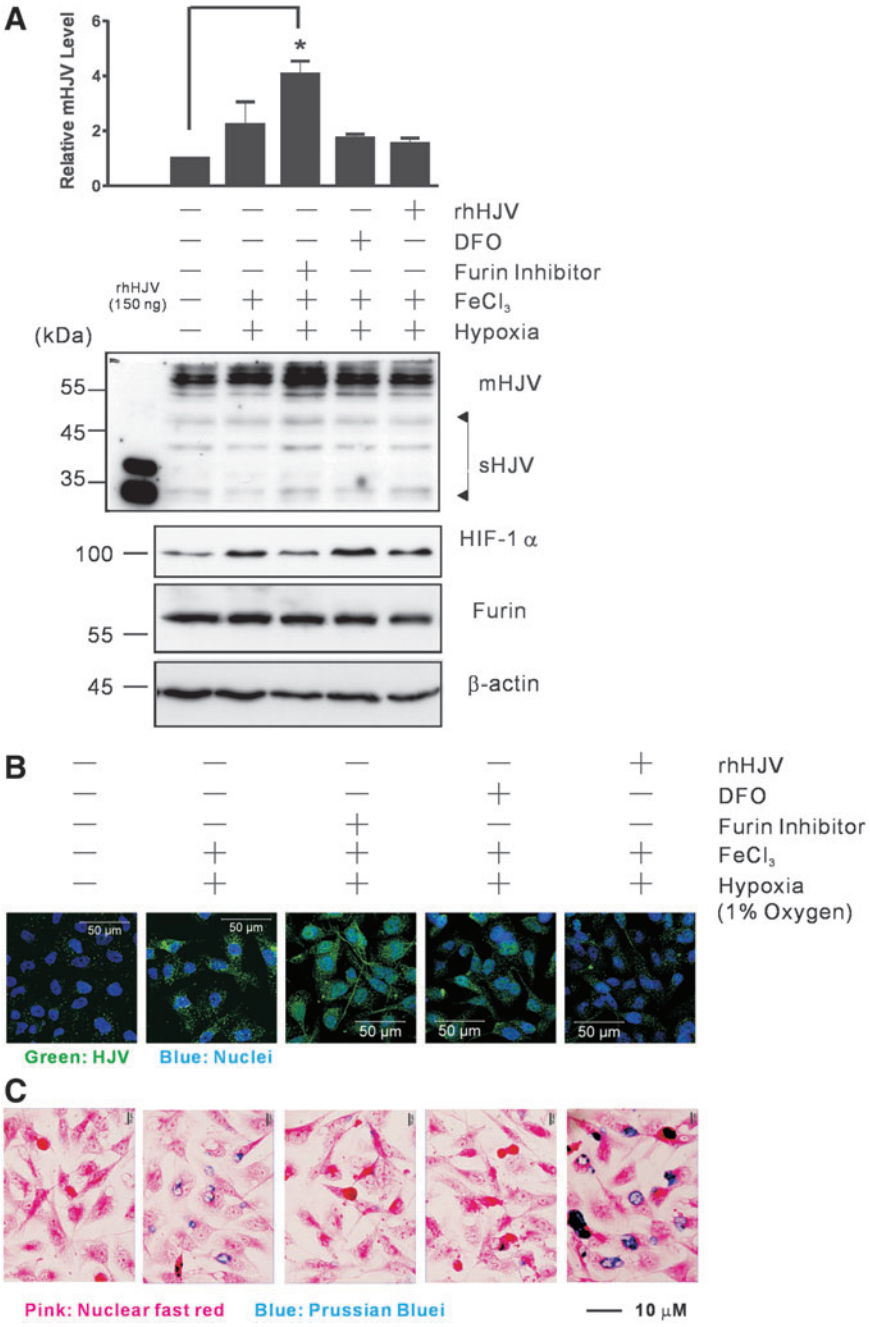

FIG. 5. The uptake and release of iron in HK2 cells after free iron stimulation under hypoxic condition. Human renal proximal renal cell lines (HK2) were pretreated with 50 μM furin inhibitor (FI), 50 μM deferoxamine (DFO), or 0.5 μg/ml recombinant human HJV protein (rhHJV) for 1 h. Then, 100 μM ferric chloride was added to the culture media under hypoxia chamber (1% oxygen) for 24 h as indicated. **(A)** Representative western blot (30 μg/well) of the cell lysate was analyzed. Typical results of five independent experiments are shown. Each experiment was normalized with the control group and 150 ng rhHJV proteins, which produced bands at 37 and 32 kDa. **(B)** Confocal microscopy was used to determine the localization of HJV (green labels) in iron-induced HK2 cells. **(C)** The cellular iron deposition of HK2 cells were examined using Prussian blue staining. Scale bars: 10 μM. *$p \leq 0.05$ *versus* control (n = 5). To see this illustration in color, the reader is referred to the web version of this article at www.liebertpub.com/ars

that HJV strongly increased in the proximal tubule in response to ischemic and rhabdomyolysis-related AKI. mHJV decreases total kidney iron, secretes hepcidin, and promotes the degradation of ferroportin, whereas sHJV does the opposite. Increased iron deposition could augment sHJV in the kidney during AKI. Therefore, plasma and urine sHJV have the potential to be an early AKI biomarker in response to the iron homeostasis during AKI.

In patients with ischemic- and rhabdomyolysis-related AKI, both urine NGAL and sHJV proteins exhibited significant expression compared with CKD and UTI. Urinary sHJV had a predictive accuracy similar to that of NGAL, a lipocalin regulating the expression of ferritin during kidney injury (23), although its utility for stratifying disease progression requires further study. We found that sHJV expression was correlated with and faster than the expression of NGAL in mouse kidney. In rhabdomyolysis-related AKI, the main cause of oxidant injury is myoglobin redox cycling and the generation of oxidized lipids (6). Urine sHJV levels increased in rhabdomyolysis patients with AKI, however, and remained with no significant change in rhabdomyolysis patients without AKI or intrinsic renal disease as glomeruopathy. Therefore, urine sHJV levels could identify between the various types and pathogeneses of AKI.

Our data also revealed that under iron overload conditions during AKI, the increased expression of the hemojuvelin-hepcidin-ferroportin pathway is an intrinsic response in kidneys that is not paralleled by reciprocal changes in liver or

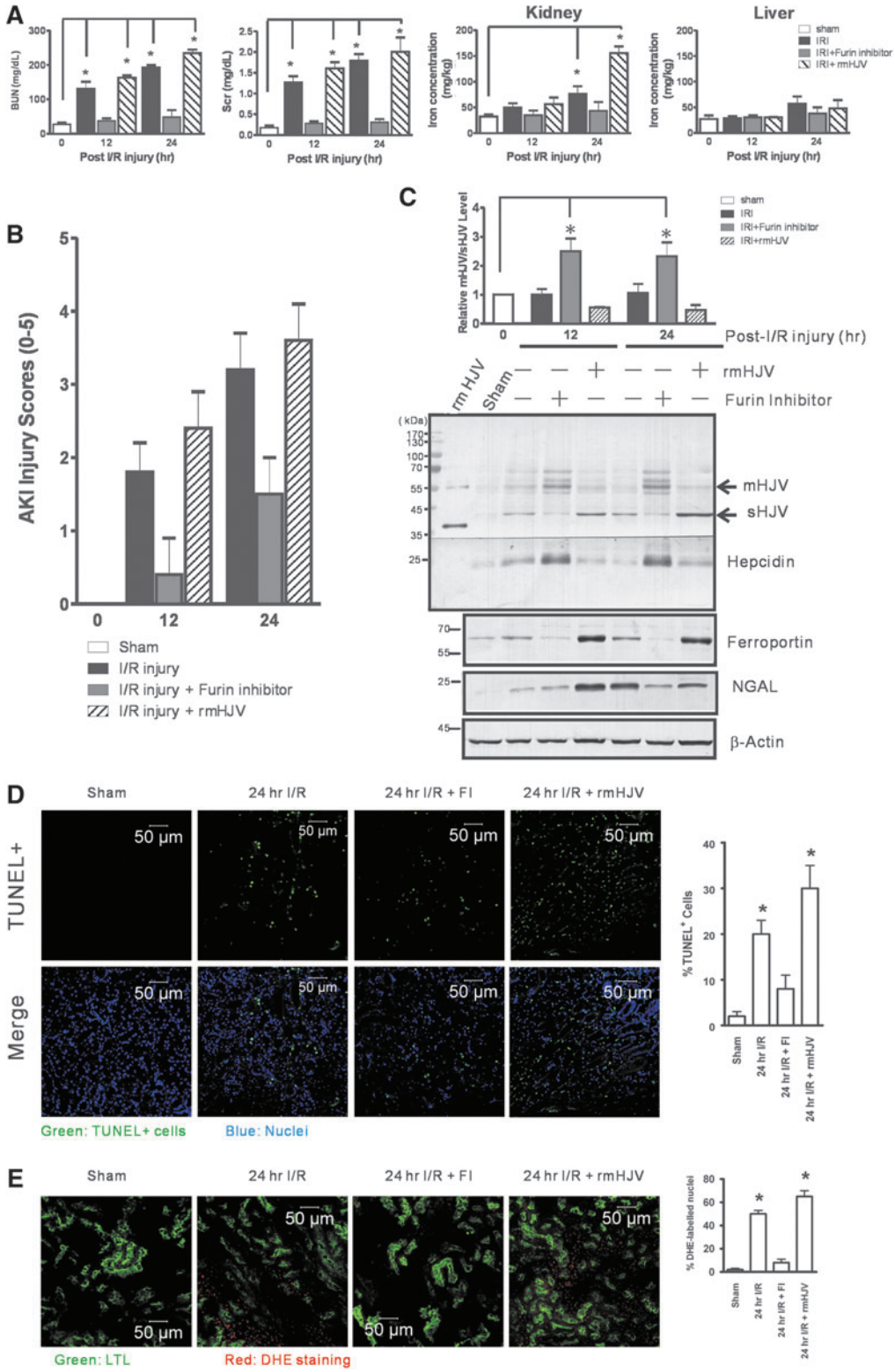

FIG. 6. Amelioration of renal I/R (AKI) injury, iron deposition, and tubular apoptosis by the FI. C57BL/6 mice were injected with 10 μg rmHJV protein, 100 μM FI, or PBS prior to unilateral renal I/R injury and sham-operated mice were used as a control. **(A)** The total kidney and liver iron concentration were measured after the mice received a kidney I/R injury. Organic iron was quantified using ICP-AES analysis. **(B)** Disease severity after I/R, evaluated by kidney injury score, improved by FI injection and aggravated by rmHJV injection. **(C)** Immunostaining of the whole kidney lysates (30 μg/well) and the ratio of mHJV/sHJV after treatment. The antibody against β-actin was used as a loading control. **(D)** Tubular apoptosis. The kidney tubules of TUNEL$^+$ apoptotic cells (green fluorescence in I/R injury) were reduced by pretreatment with an FI, as determined by fluorescent staining. The same field was merged with a DAPI-stained image, showing the nucleus as a counter stain (blue). Scale bars: 50 μM. **(E)** *In situ* localization of reactive oxygen species (ROS). Dihydroethidium (DHE) fluorescent analysis was used for evaluation of ROS. The same field was merged with an FITC-labeled lotus tetragonolobus lectin (LTL), which is a proximal tubular marker for histological co-localization. Scale bars: 50 μM. *$p \leq 0.05$ *versus* control (n = 10). To see this illustration in color, the reader is referred to the web version of this article at www.liebertpub.com/ars

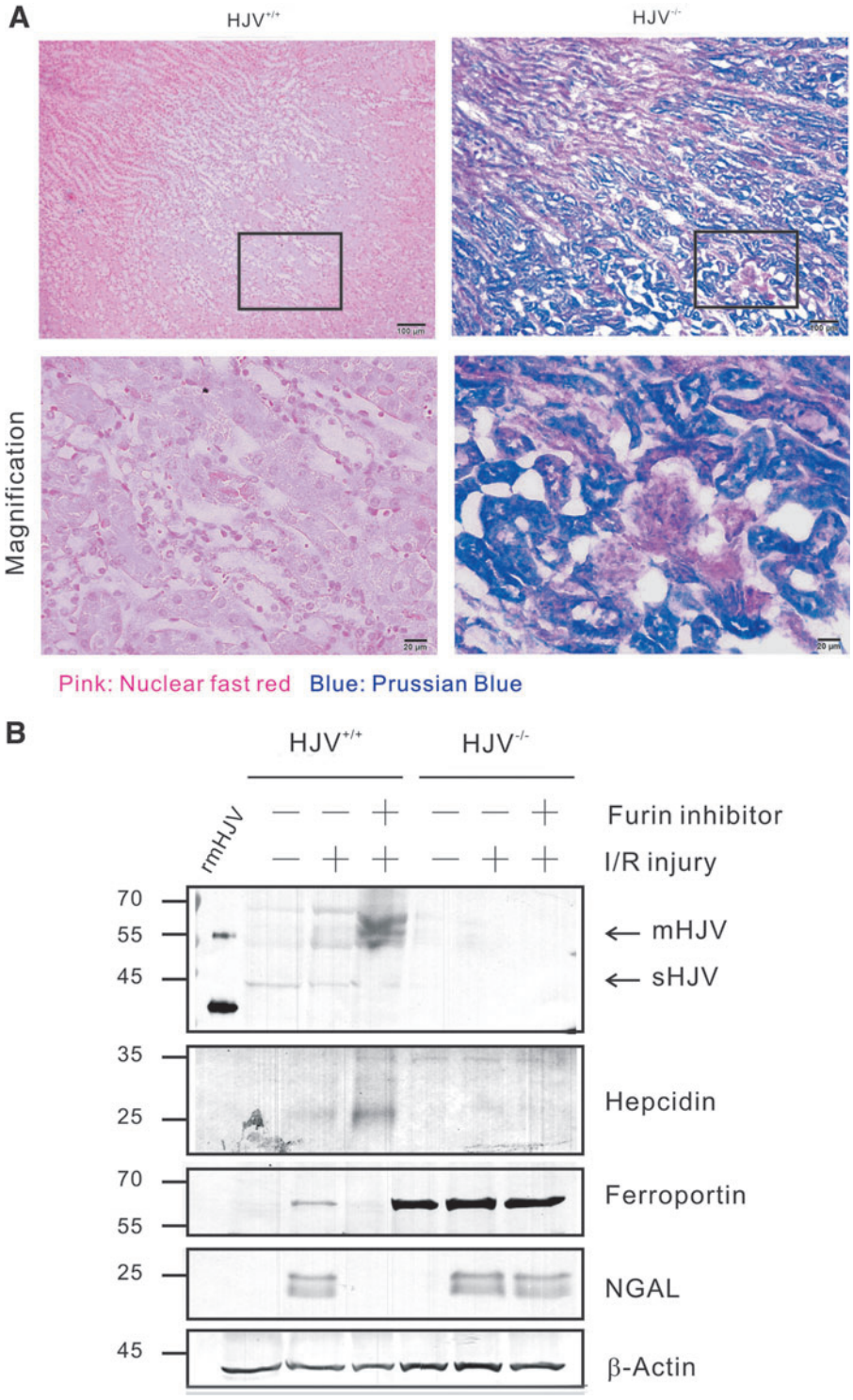

FIG. 7. FI ameliorated renal I/R (AKI) injury *via* HJV-mediated mechanism. (A) Iron accumulated in hemojuvelin knockout ($HJV^{-/-}$) mice. Kidney iron was detected by Prussian blue staining. **(B)** $HJV^{+/+}$ or $HJV^{-/-}$ mice received FI or PBS prior to unilateral renal I/R injury and sham-operation as control. Mice were sacrificed at 24 h after I/R injury. The expression levels of HJV, hepcidin, ferroportin, NGAL, and β-actin in kidney were determined by western analysis. To see this illustration in color, the reader is referred to the web version of this article at www.liebertpub.com/ars

muscle iron. In hepatocytes, sHJV inversely reflects the systemic iron load or signals the iron requirements for myoglobin synthesis and is a useful biomarker in iron dysregulation (20). Therefore, the release of sHJV is a tissue-specific mechanism (33), signaling the local iron requirements of hypoxic kidneys independently of the oxygen status of the liver or muscle. The same also occurs in HK2 cells infused with catalytic iron. Under iron-mediated stress (13), the mHJV increased. However, addition of the FI could augment the expression of HJV in terms of the renoprotective molecule under iron overload and hypoxic conditions (17).

We further postulate that the augmentation of mHJV in these segments of the nephron after renal ischemia leads to the downregulation of ferroportin, linking free iron in the tissues and the resulting perpetuation of tubular injury. Likewise, increased mHJV enhanced hepcidin production, but rmHJV

(sHJV) did the opposite. rmHJV injection increased the kidney iron concentration, counterbalanced the hepcidin activity and therefore blocked the degradation of ferroportin, and then aggravated disease progression. These findings support our main result that the hemojuvelin-hepcidin-ferroportin axis is one of the most highly expressed messengers and proteins following AKI.

We have shown the loss of mHJV is associated with iron deposition in the kidney injured by I/R. In the early stages, the degraded form of HJV (sHJV) appeared faster than mHJV in injured kidneys and could be detected in urine. The rapidly induced sHJV could cause iron deposition in the kidneys (1), especially during AKI. However, the gradually increased mHJV might play a protective role in response to iron homeostasis. This concept is supported by our animal model, which indicated that when the proportion of kidney mHJV exceeded that of sHJV after the acute stage, iron deposition in the kidney decreased (Fig. 2G).

It appears that the FI inhibited sHJV and augmented mHJV. HJV undergoes complicated post-translational processing in an iron-dependent manner, and an increased mHJV/sHJV ratio could augment the hepcidin response, prevent iron deposition, and decrease apoptosis following kidney injury. Consistent with our findings in the kidney, prior work showed that mHJV and sHJV play reciprocal functions, suggesting binding competition between sHJV and mHJV, in response to body iron status *via* cleavage by the furin protease in hepatocytes (33).

Intriguingly, endogenous furin is universal in many tissues, whereas elevated furin expression is associated with hypoxia stress (21). The furin promoter possesses the element binding sites for the HIF-1 transcription complex. Our result showed FI is efficacious to stabilize HIF-1alpha and reduce iron-mediated kidney ischemia. Therefore, furin protease plays a pivotal role in modulating iron-mediated kidney injury.

After injection of the FI, kidney iron deposition decreased, tubule apoptosis was reduced, and AKI markers such as NGAL decreased (Fig. 6B, C). It has recently been reported that BMP signaling, with HJV as a coreceptor, regulates the expression of hepcidin in the liver (45). The pretreated FI or DFO reduced the generation of sHJV and further protected against kidney injury during the iron-mediated injury of HK2 cells. However, after renal I/R injury, FI could not improve the injury of I/R among $HJV^{-/-}$ mice as those in wild-type mice (Fig. 7). Results from mice protected against anthrax toxemia by systemic treatment with FIs suggest that the application might have acceptable side effects (31). In light of this, kidney injury could be modulated by the hemojuvelin-hepcidin-ferroportin axis and the furin inhbitor could, at least partly, reduce kidney injury by stabilizing iron deposition.

In conclusion, our findings reveal a novel role in iron modulation for kidney HJV during AKI. The endogenous HJV in kidneys is highly expressed in the renal tubule during AKI, and the urinary sHJV could be an early biomarker in response to AKI injury. Elevation of the mHJV plays a pivotal role in crosstalk with kidney iron contents, whereas the FI diminishes the generation of sHJV and further protects against AKI. Our results reinforce the view that the FI could stabilize HIF-1, augment the reciprocal change of HJV, repress apoptosis, degrade ferroportin, and further decrease iron deposition in mouse kidney during AKI.

Materials and Methods

Human specimens

All patients were registered in the National Taiwan University Hospital Study Group on Acute Renal Failure (NSARF) (16, 39, 40, 42). The database was constructed for quality assurance in one medical center (National Taiwan University Hospital in Taipei, Taiwan) and its three branch hospitals in different cities. During the whole study period, 5-ml samples of urine were collected from each patient undergoing cardiac surgery, at 3 h after operation. The definition of AKI was based on the Acute Kidney Injury Network (AKIN) criteria and has been well validated in cardiac surgery patients for in-hospital mortality predictions. Paraffin-embedded human kidney sections were obtained from the NTUH Tissue Resource Center under an IRB-approved protocol. This study was approved by the Institutional Review Board of the National Taiwan University Hospital, Taipei, Taiwan (No. 201105047RC) (Clinical Trials. Gov. Number, NCT01503710). All participants signed a written informed consent before inclusion in the study.

Preparations of urine samples

The urine samples collected in separated polypropylene tubes (BD Biosciences) containing sodium azide (Sigma-Aldrich) were stored at −80°C until they were used. The pooled urine samples were concentrated using an Amicon Ultra-15 centrifugal filter unit (Amersham Biosciences), passed through a PD-10 desalting column (Amersham Biosciences), and eluted with 10 m*M* PBS, pH 7.4. The eluted fractions containing proteins were added to two volumes of cold 20% TCA in acetone (Merck) for protein precipitation. The mixture was stored overnight at −20°C until use, and the pellet was obtained by centrifugation at 10,000 *g* at 4°C for 15 min. The pellet was vacuum dried on a SpeedVac (SC110).

2-DE and MALDI

The pellets were rehydrated in 2-DE sample buffer (8 *M* urea, 2% Pharmalyte, pH 3–10, 60 m*M* DTT, 0.5% Triton X-100, and traces of bromophenol blue). A 1 mg aliquot of the pellet was mixed with 120 μl of 2-DE sample buffer (8 *M* urea, 2% Pharmalyte, pH 3–10, 60 m*M* DTT, 0.5% Triton X-100, and traces of bromophenol blue) and run as the first dimension of the 2-DE on an 11 cm Immobiline DryStrip, pH 3–10 (GE Healthcare). In the second dimension, the proteins were separated in 12.5% SDS-PAGE gels and stained using Coomassie Brilliant Blue R250. For the mass spectrometric identification, each individual spot was cut out and digested with trypsin (Promega), as described previously (19). The resulting peptides were sequentially extracted with 1% TFA and 0.1% TFA/50% ACN, and the pooled extracts were lyophilized and resuspended in 10 μl of 0.1% TFA. The peptides were characterized using a Qstar XL Q-TOF mass spectrometer (Applied Biosystems) coupled to an UltiMateTM Nano LCsystem (Dionex/LC Packings). The protein identification generated from the MS/MS spectra were uploaded to the MASCOT search engine v2.2 (Matrix Science).

Measurements of urinary NGAL and HJV

The urine samples collected in separate polypropylene tubes containing sodium azide were stored at −80°C until

use. Each specimen was centrifuged at 800 *g* at 4°C for 5 min, and the supernatant was removed for an ELISA assay. The urinary NGAL level was determined using a human lipocalin-2/NGAL ELISA kit (R&D Systems), and the HJV level was determined using a human hemojuvelin ELISA kit (USCN). All operations were performed according to the manufacturer's protocols, and each assay was performed in duplicate.

Study animals

The animal protocols and procedures were handled in accordance with the guidelines of the National Taiwan University College of Medicine and College of Public Health for the care and use of laboratory animals (NIH publication No. 86-23, revised 1985) with Institutional Animal Care and Use Committee (IACUC) approval. HJV knockout mice (129S-Hfe2^{tm1Nca}/J), maintained on an inbred 129S6/SvEvTac background, were purchased from the Jackson Laboratory which is donated by Dr. Nancy Andrews (Duke University).

Unilateral renal I/R

Male Wistar rats (110 ± 15 g), C57BL/6 mice (20 ± 2 g) or Hjv$^{-/-}$ mice were briefly anesthetized with anesthesia cocktails (80 mg/kg ketamine plus 100 mg/kg xylazine) *via* i.p. injection and were placed on a heating pad to maintain core temperature of 37°C. The kidneys were exposed *via* an abdominal section; the left kidney was clamped by a microaneurysm clip for 45 min, and the right kidney was removed as previously reported (9, 23, 43). Reperfusion was confirmed visually upon release of the clamp. As a control, sham-operated animals were subjected to the same surgical procedure except the left renal pedicles were not clamped. The surgical wounds were closed, and the animals were given 1 ml of warm saline (i.p.) and remained in a warm incubator until they regained consciousness. The urine was collected by bladder massage and stored at −80°C until use.

Rhabdomyolysis-associated ATN

ATN was induced in male C57BL/6 mice by an i.m. injection with 50% glycerol (Amresco) solution in water (10 ml/kg body/wt) (27). In brief, the animals (body weight 20 ± 2 g) were injected with glycerol into the left and right hind femoral muscles. The animals received 160 ± 10 μl of 50% glycerol/g body weight on average (Supplementary Fig. S2).

Drug administration

Before 1 h of the renal I/R surgery, the mice received an i.v. injection of a volume of 100 μl PBS with 10 μg (R&D Systems), 100 μ*M* FI II (hexa-D-arginine; Merck) or PBS only (30, 31).

Renal function

Renal function was assessed by measurements of the BUN (BUN-PIII dri-chem slide; FUJIFILM) and Scr (CRE-PIII dri-chem slide; FUJIFILM) levels.

Measurements of plasma HJV

The mouse plasma HJV was measured using a mouse hemojuvelin ELISA kit (USCN) according to the manufacturer's protocols.

Injury scores for kidneys sections

Quantitative evaluation of injury scores are defined based on cast formation, tubular dilation, and tubular necrosis as described by EI-AchKar *et al.* (10) and then given an injury score from 0 to 5 for each features. Ten high-power fields per section were counted for tubular injury.

Histological analysis

Mouse kidneys were perfused with cold PBS to remove blood and fixed in 10% formaldehyde for paraffin embedding or transferred to 30% sucrose overnight and embedded in an OCT compound (Sakura Finetek) for frozen sections. The sections of paraffin-embedded tissue were stained with H&E or processed for IHC with a non-biotin-amplified method (Novolink; Novocastra Laboratories). To determine renal tubular apoptosis, the paraffin-embedded kidney sections were stained using terminal deoxynucleotidyl transferase dUTP nick-end labeling (TUNEL) with an *in situ* cell death detection kit (Roche). Slides were analyzed using LSM 510 confocal microscopy (Carl Zeiss). For *in situ* detection of ROS, dihydroethidium (DHE) staining (Sigma-Aldrich) was performed on frozen kidney sections (6 μm). Kidney sections were incubated with 6.3 μ*M* DHE in Kreb's/HEPES buffer and applied at 37°C for 30 min in a humidified chamber protected from light. Confocal images were analyzed by morphometric analysis of pixels per nucleus.

Cell culture, iron induction, immunoprecipitation, and Prussian blue staining

Human renal proximal renal cells (BCRC60097, Bioresource Collection and Research Center, BCRC) were grown and passaged in culture flasks containing culture medium (Keratinocyte-Serum-free Medium containing 5 ng/ml recombinant epidermal growth factor and 40 μg/ml bovine pituitary extract) at 37°C in a 100% humidified atmosphere with 5% CO_2 (29).

Iron induction

The HK2 cells grown on 6 cm plates were collected when confluent. Pretreatment with 100 μ*M* FI II (Merck) (Supplementary Fig. S8), 100 μ*M* DFO (Sigma-Aldrich), or 0.5 μg/ml rhHJV (R&D) was performed for 1 h. The cells were then added to 100 μ*M* $FeCl_3$ (Sigma-Aldrich) for 24 h.

Immunoprecipitation of culture media

For immunoprecipitation, 1 ml of the culture media was incubated with 1 μg of anti-HJV antibody for 1 h and 50 μl of pre-equilibrated TrueBlot anti-mouse Ig IP beads slurry overnight at 4°C with continuous mixing (eBioscience). The beads were centrifuged at 2500 *g* at 4°C for 30 s. The supernatant was removed, and the beads were washed five times at 4°C with 1 ml of wash buffer (50 m*M* Tris-HCl, pH 8.0, 150 m*M* NaCl, and 1% NP-40). The proteins were eluted from beads and aspirated from the supernatant by adding SDS sample buffer with 50 m*M* DTT and heating to 100°C for 10 min and were then used for SDS-PAGE.

Prussian blue staining

The cells were fixed with 2% formaldehyde for 30 min and then washed with de-ionized water. Prussian blue staining was performed according to Perls' reaction using an iron stain

kit (ScyTek Laboratories). The image of iron accumulation was obtained using a Nikon digital camera Dx/m/1200 and Lucia software (Laboratory Imaging, Ltd.). The section was quantified at 100× magnification.

Iron quantification

The kidney and liver from each mouse were digested with 0.5, 1.0, and 1.0 ml of mixed acid ($HNO_3/HC10_4 = 122$ 5:1, v/v), and the solutions were diluted to 5, 10, and 10 ml, respectively, with doubly distilled water. The concentrations of iron (Fe) in these organs were simultaneously determined using ICP-AES (18) (Jarrell-Ash Model 975 Plasma Atomcomp).

Protein extraction and western blot

For the total protein extraction, lysates from cells, kidney, or liver dissolved in RIPA buffer containing a protease inhibitor cocktail (Roche) were quantitated using the BCA protein assay reagent (Pierce Biotechnology) as previously described (41). A 30 μg sample of protein from each specimen was separated using SDS-PAGE and transferred onto PVDF membranes (Millipore). The rabbit anti-HJV polyclonal antibody, rabbit anti-ferroportin polyclonal antibody, mouse anti-HJV monoclonal antibody, and anti-hepcidin antibody were purchased from AVNOVA. The mouse anti-actin monoclonal antibody and the rabbit anti-furin polyclonal antibody were purchased from Santa Cruz, the goat anti-NGAL polyclonal antibody was purchased from R&D, and the mouse anti-HIF-1alpha monoclonal antibody was purchased from Millipore. After the membrane was washed thrice with PBST, the enzyme activity on the blot was visualized using NBT/BCIP (Promega), according to the manufacturer's instructions (Supplementary Fig. S5 and S6).

Statistical analysis

All data were described as the mean ± SD. Different results among groups were compared using the Kruskal–Wallis one-way analysis of variance on Ranks (ANOVA) or the two-tailed *T*-test. The results were considered significant when $p < 0.05$.

Acknowledgments

The authors would like to thank the staff of the Second and the Seventh Core Lab of the Department of Medical Research in the National Taiwan University Hospital for technical assistance. This study was supported by the Ta-Tung Kidney Foundation, Taiwan National Science Council (grant NSC 96-2314-B-002-164, NSC 96-2314-B-002-033-MY3, NSC 97-2314-B-002-155-MY2, NSC 98-2314-B-002-155-MY4, NSC 100-2314-B-002-147-MY3, and NSC 101-2314-B-002-085-MY3), and the National Taiwan University Hospital grant, NTUH 098-001177, NTUH 100-001667, and NTUH-101-062.

Author Disclosure Statement

No competing financial interests exist.

References

1. Babitt JL, Huang FW, Xia Y, Sidis Y, Andrews NC, and Lin HY. Modulation of bone morphogenetic protein signaling *in vivo* regulates systemic iron balance. *J Clin Invest* 117: 1933–1939, 2007.
2. Baliga R, Ueda N, and Shah SV. Increase in bleomycin-detectable iron in ischemia-reperfusion injury to rat kidneys. *Biochem J* 291: 901–905, 1993.
3. Baliga R, Zhang ZW, Baliga M, and Shah SV. Evidence for cytochrome P-450 as a source of catalytic iron in myoglobinuric acute renal failure. *Kidney Int* 49: 362–369, 1996.
4. This reference has been deleted.
5. Baliga R, Zhang ZW, and Shah SV. Role of cytochrome P-450 in hydrogen peroxide-induced cytotoxicity to LLC-PK1 cells. *Kidney Int* 50: 1118–1124, 1996.
6. Boutaud O, Roberts LJ, 2nd. Mechanism-based therapeutic approaches to rhabdomyolysis-induced renal failure. *Free Radic Biol Med* 51: 1062–1067, 2011.
7. Coca SG. Acute kidney injury in elderly persons. *Am J Kidney Dis* 56: 122–131, 2010.
8. Devarajan P, Krawczeski CD, Nguyen MT, Kathman T, Wang Z, and Parikh CR. Proteomic identification of early biomarkers of acute kidney injury after cardiac surgery in children. *Am J Kidney Dis* 56: 632–642, 2010.
9. Duffield JS, Park KM, Hsiao LL, Kelley VR, Scadden DT, Ichimura T, and Bonventre JV. Restoration of tubular epithelial cells during repair of the postischemic kidney occurs independently of bone marrow-derived stem cells. *J Clin Invest* 115: 1743–1755, 2005.
10. El-Achkar TM, Wu XR, Rauchman M, McCracken R, Kiefer S, and Dagher PC. Tamm-Horsfall protein protects the kidney from ischemic injury by decreasing inflammation and altering TLR4 expression. *Am J Physiol Renal Physiol* 295: F534–F544, 2008.
11. Haase M, Bellomo R, and Haase-Fielitz A. Novel biomarkers, oxidative stress, and the role of labile iron toxicity in cardiopulmonary bypass-associated acute kidney injury. *J Am Coll Cardiol* 55: 2024–2033, 2010.
12. Halliwell B and Gutteridge JMC. Role of free-radicals and catalytic metal-ions in human-disease—an overview. *Method Enzymol* 186: 1–85, 1990.
13. Harding C, Heuser J, and Stahl P. Receptor-mediated endocytosis of transferrin and recycling of the transferrin receptor in rat reticulocytes. *J Cell Biol* 97: 329–339, 1983.
14. Ho J, Lucy M, Krokhin O, Hayglass K, Pascoe E, Darroch G, Rush D, Nickerson P, Rigatto C, and Reslerova M. Mass spectrometry-based proteomic analysis of urine in acute kidney injury following cardiopulmonary bypass: a nested case-control study. *Am J Kidney Dis* 53: 584–595, 2009.
15. Huang FW, Pinkus JL, Pinkus GS, Fleming MD, and Andrews NC. A mouse model of juvenile hemochromatosis. *J Clin Invest* 115: 2187–2191, 2005.
16. Huang TM, Wu VC, Young GH, Lin YF, Shiao CC, Wu PC, Li WY, Yu HY, Hu FC, Lin JW, Chen YS, Lin YH, Wang SS, Hsu RB, Chang FC, Chou NK, Chu TS, Yeh YC, Tsai PR, Huang JW, Lin SL, Chen YM, Ko WJ, Wu KD, and Grp NTUHS. Preoperative proteinuria predicts adverse renal outcomes after coronary artery bypass grafting. *J Am Soc Nephrol* 22: 156–163, 2011.
17. Ishizaka N, Saito K, Furuta K, Matsuzaki G, Koike K, Noiri E, and Nagai R. Angiotensin II-induced regulation of the expression and localization of iron metabolism-related genes in the rat kidney. *Hypertens Res* 30: 195–202, 2007.
18. Kingston HM and Jassie LB. Microwave acid sample decomposition for elemental analysis. *J Res Natl Inst Stan* 93: 269–274, 1988.
19. Lee IN, Chen CH, Sheu JC, Lee HS, Huang GT, Chen DS, Yu CY, Wen CL, Lu FJ, and Chow LP. Identification of complement C3a as a candidate biomarker in human chronic

hepatitis C and HCV-related hepatocellular carcinoma using a proteomics approach. *Proteomics* 6: 2865–2873, 2006.
20. Lin L, Goldberg YP, and Ganz T. Competitive regulation of hepcidin mRNA by soluble and cell-associated hemojuvelin. *Blood* 106: 2884–2889, 2005.
21. McMahon S, Grondin F, McDonald PP, Richard DE, and Dubois CM. Hypoxia-enhanced expression of the proprotein convertase furin is mediated by hypoxia-inducible factor-1: impact on the bioactivation of proproteins. *J Biol Chem* 280: 6561–6569, 2005.
22. Mehta RL, Kellum JA, Shah SV, Molitoris BA, Ronco C, Warnock DG, and Levin A. Acute Kidney Injury Network: report of an initiative to improve outcomes in acute kidney injury. *Crit Care* 11: R31, 2007.
23. Mori K, Lee HT, Rapoport D, Drexler IR, Foster K, Yang J, Schmidt-Ott KM, Chen X, Li JY, Weiss S, Mishra J, Cheema FH, Markowitz G, Suganami T, Sawai K, Mukoyama M, Kunis C, D'Agati V, Devarajan P, and Barasch J. Endocytic delivery of lipocalin-siderophore-iron complex rescues the kidney from ischemia-reperfusion injury. *J Clin Invest* 115: 610–621, 2005.
24. Moriguchi J, Ezaki T, Tsukahara T, Furuki K, Fukui Y, Okamoto S, Ukai H, Sakurai H, Shimbo S, and Ikeda M. Comparative evaluation of four urinary tubular dysfunction markers, with special references to the effects of aging and correction for creatinine concentration. *Toxicol Lett* 143: 279–290, 2003.
25. Niederkofler V, Salie R, and Arber S. Hemojuvelin is essential for dietary iron sensing, and its mutation leads to severe iron overload. *J Clin Invest* 115: 2180–2186, 2005.
26. Paller MS and Hedlund BE. Role of iron in postischemic renal injury in the rat. *Kidney Int* 34: 474–480, 1988.
27. Perin L, Sedrakyan S, Giuliani S, Da Sacco S, Carraro G, Shiri L, Lemley KV, Rosol M, Wu S, Atala A, Warburton D, and De Filippo RE. Protective effect of human amniotic fluid stem cells in an immunodeficient mouse model of acute tubular necrosis. *PLoS One* 5: e9357, 2010.
28. Rodriguez Martinez A, Niemela O, and Parkkila S. Hepatic and extrahepatic expression of the new iron regulatory protein hemojuvelin. *Haematologica* 89: 1441–1445, 2004.
29. Ryan MJ, Johnson G, Kirk J, Fuerstenberg SM, Zager RA, and Torok-Storb B. HK-2: an immortalized proximal tubule epithelial cell line from normal adult human kidney. *Kidney Int* 45: 48–57, 1994.
30. Sarac MS, Cameron A, and Lindberg I. The furin inhibitor hexa-D-arginine blocks the activation of *Pseudomonas aeruginosa* exotoxin A *in vivo*. *Infect Immun* 70: 7136–7139, 2002.
31. Sarac MS, Peinado JR, Leppla SH, and Lindberg I. Protection against anthrax toxemia by hexa-D-arginine *in vitro* and *in vivo*. *Infect Immun* 72: 602–605, 2004.
32. This reference has been deleted.
33. Silvestri L, Pagani A, and Camaschella C. Furin-mediated release of soluble hemojuvelin: a new link between hypoxia and iron homeostasis. *Blood* 111: 924–931, 2008.
34. Silvestri L, Pagani A, Fazi C, Gerardi G, Levi S, Arosio P, and Camaschella C. Defective targeting of hemojuvelin to plasma membrane is a common pathogenetic mechanism in juvenile hemochromatosis. *Blood* 109: 4503–4510, 2007.
35. Vincent SH, Grady RW, Shaklai N, Snider JM, and Muller-Eberhard U. The influence of heme-binding proteins in heme-catalyzed oxidations. *Arch Biochem Biophys* 265: 539–550, 1988.
36. Waikar SS, Liu KD, and Chertow GM. Diagnosis, epidemiology and outcomes of acute kidney injury. *Clin J Am Soc Nephrol* 3: 844–861, 2008.
37. Walker PD and Shah SV. Evidence suggesting a role for hydroxyl radical in gentamicin-induced acute renal failure in rats. *J Clin Invest* 81: 334–341, 1988.
38. Woollard KJ, Sturgeon S, Chin-Dusting JP, Salem HH, and Jackson SP. Erythrocyte hemolysis and hemoglobin oxidation promote ferric chloride-induced vascular injury. *J Biol Chem* 284: 13110–13118, 2009.
39. Wu VC, Ko WJ, Chang HW, Chen YS, Chen YW, Chen YM, Hu FC, Lin YH, Tsai PR, and Wu KD. Early renal replacement therapy in patients with postoperative acute liver failure associated with acute renal failure: Effect on postoperative outcomes. *J Am Coll Surgeons* 205: 266–276, 2007.
40. Wu VC, Ko WJ, Chang HW, Chen YW, Lin YF, Shiao CC, Chen YM, Chen YS, Tsai PR, Hu FC, Wang JY, Lin YH, Wu KD, and Re NTUSIA. Risk factors of early redialysis after weaning from postoperative acute renal replacement therapy. *Intensive Care Med* 34: 101–108, 2008.
41. Wu VC, Lo SC, Chen YL, Huang PH, Tsai CT, Liang CJ, Kuo CC, Kuo YS, Lee BC, Wu EL, Lin YH, Sun YY, Lin SL, Chen JW, Lin SJ, Wu KD, and Grp TS. Endothelial progenitor cells in primary aldosteronism: a biomarker of severity for aldosterone vasculopathy and prognosis. *J Clin Endocrinol Metab* 96: 3175–3183, 2011.
42. Wu VC, Wang CH, Wang WJ, Lin YF, Hu FC, Chen YW, Chen YS, Wu MS, Lin YH, Kuo CC, Huang TM, Chen YM, Tsai PR, Ko WJ, Wu KD, and Grp NS. Sustained low-efficiency dialysis versus continuous veno-venous hemofiltration for postsurgical acute renal failure. *Am J Surg* 199: 466–476, 2010.
43. Wu VC, Young GH, Huang PH, Lo SC, Wang KC, Sun CY, Liang CJ, Huang TM, Chen JH, Chang FC, Chen YL, Kuo YS, Chen JB, Chen JW, Chen YM, Ko WJ, Wu KD, The Ng. In acute kidney injury, indoxyl sulfate impairs human endothelial progenitor cells: modulation by statin. *Angiogenesis* 16: 609–624 2013.
44. Zhang AS, West AP, Jr., Wyman AE, Bjorkman PJ, and Enns CA. Interaction of hemojuvelin with neogenin results in iron accumulation in human embryonic kidney 293 cells. *J Biol Chem* 280: 33885–33894, 2005.
45. Zhang AS, Yang F, Wang J, Tsukamoto H, and Enns CA. Hemojuvelin-neogenin interaction is required for bone morphogenic protein-4-induced hepcidin expression. *J Biol Chem* 284: 22580–22589, 2009.

Address correspondence to:
Dr. Wen-Je Ko
Department of Surgery
National Taiwan University Hospital
7 Chung-Shan South Road
Zhong-Zheng District
Taipei 100
Taiwan

E-mail: kowj@ntu.edu.tw

Dr. Vin-Cent Wu
Division of Nephrology
Department of Internal Medicine
National Taiwan University Hospital
7 Chung-Shan South Road
Taipei 100
Taiwan

E-mail: q91421028@ntu.edu.tw

Date of first submission to ARS Central, April 17, 2013; date of final revised submission, July 9, 2013; date of acceptance, July 31, 2013.

Abbreviations Used

2-DE = two-dimensional electrophoresis
AKI = acute kidney injury
ATN = acute tubular necrosis
BUN = blood urea nitrogen
CKD = chronic kidney disease
DFO = deferoxamine
DHE = dihydroethidium
FI = furin inhibitor
H&E = hematoxylin and eosin stain
HIF-1 = hypoxic-induced factor-1
$HJV^{-/-}$ mice = hemojuvelin knockout mice
HK2 = human proximal tubular cell
ICP-AES = inductively coupled plasma atomic emission spectroscopy
IHC = immunohistochemical
IP = immunoprecipitation
mHJV = membrane-bound hemojuvelin
NGAL = neutrophil gelatinase-associated lipocalin
NSARF = National Taiwan University Hospital Study Group on Acute Renal Failure
PAS = periodic acid-Schiff
rhHJV = recombinant human hemojuvelin protein
rmHJV = recombinant mouse hemojuvelin protein
ROS = reactive oxygen species
Scr = serum creatinine
sHJV = soluble hemojuvelin
TCA = trichloroacetic acid
UTI = urinary tract infection